ENGINEERING

On-skin paintable biogel for long-term high-fidelity electroencephalogram recording

Chunya Wang, Haoyang Wang, Binghao Wang, Hiroo Miyata, Yan Wang, Md Osman Goni Nayeem, Jae Joon Kim, Sunghoon Lee, Tomoyuki Yokota, Hiroshi Onodera, Takao Someya*

Long-term high-fidelity electroencephalogram (EEG) recordings are critical for clinical and brain science applications. Conductive liquid-like or solid-like wet interface materials have been conventionally used as reliable interfaces for EEG recording. However, because of their simplex liquid or solid phase, electrodes with them as interfaces confront inadequate dynamic adaptability to hairy scalp, which makes it challenging to maintain stable and efficient contact of electrodes with scalp for long-term EEG recording. Here, we develop an on-skin paintable conductive biogel that shows temperature-controlled reversible fluid-gel transition to address the abovementioned limitation. This phase transition endows the biogel with unique on-skin paintability and in situ gelatinization, establishing conformal contact and dynamic compliance of electrodes with hairy scalp. The biogel is demonstrated as an efficient interface for long-term high-quality EEG recording over several days and for the high-performance capture and classification of evoked potentials. The paintable biogel offers a biocompatible and long-term reliable interface for EEG-based systems.

INTRODUCTION

Highly effective epidermal recording of electrophysiological signals with long-term reliability is of great importance for clinical diagnostics/therapeutics and brain science research (*1*–*3*). To achieve long-term high-quality electrophysiological recording, the bioelectrode interfacing with soft skin tissue must meet high requirements, such as good conformality, favorable mechanical interaction, and long-term reliability (*4*). Compared to electrophysiological recording through nonhairy skin [e.g., electrocardiography (ECG) and electromyography (EMG)], it is more difficult for long-term reliable electroencephalogram (EEG) recording, because EEG signals are weaker (with micro-volt signal amplitude) and dense hairs can cause interference to the efficient interfacing of the electrodes with the scalp (*5*). One prerequisite for reliable EEG recording is to construct a stable interface between the electrodes and the scalp. Ionically conductive liquid-like gels and grease-like pastes have been commonly applied as the gold-standard reliable interfaces for high-quality EEG monitoring through hairy scalp, because their nonsolid state provides them the ability to penetrate through hairs to form conformal contact with the scalp, ensuring electrical compatibility and conformability between the electrodes and scalp (*6*). The nonsolid phase of conventional gels/pastes leads to their inferior cohesiveness and weak mechanical interaction, making them susceptible to dislocation/spreading (short-circuit possibility for adjacent electrodes) and making it inevitable for fixation (mesh cap or chin strap) to secure the electrodes onto the head.

Soft solid-like hydrogels with tissue-like mechanical properties, ionic conductivity, and epidermal hydration effectivity have been studied as alternative candidate interfacing materials for EEG recording, because they provide a possible material approach to addressing the spreading issue of conventional gels/pastes owing to their preformed solid phases (*5*, *7*–*9*). Nevertheless, the preformed morphologies of the solid hydrogels obstruct their conformal contact with the hairy scalp, resulting in the need for an additional mechanical fixture (pressure intervention) to achieve reliable contact of soft hydrogels with scalp and to avoid electrode detachment (*7*, *8*). For the recording of EEG signals for long-term duration, another critical limitation for conventional gel/paste interfaces concerns their dry-out susceptibility, as this leads to signal deterioration when monitoring is performed for more than several hours (*10*, *11*). Electrolyte-permeable materials with porous structures have been developed with electrolyte solution and bulky electrolyte reservoirs to provide reliable interfaces for long-term EEG monitoring, because the electrolyte can be released from the reservoir to hydrate the scalp by applying pressure or using capillary force (*6*). A stringent geometry design for the electrodes and cumbersome supporting systems are usually indispensable to achieve the efficient contact of the electrodes with the hairy scalp and to accomplish the release of electrolyte. Very recently, a homeostatic biointerface based on a porous cellulose membrane swollen by saline solution was constructed with a bulky solution reservoir and provided continuous EEG signal recording for more than 8 hours (*12*). Besides, dry contact electrodes such as ultrathin kirigami conductor, ultrathin epidermal electrode, elastic sponge electrode, and flexible claw-like electrode have been developed as another possible technique for user-friendly and long-term EEG detection (*11*, *13*–*15*). Dry electrodes with ultrathin structure are only appropriate for the capture of EEG on nonhairy skin location (*11*, *15*, *16*).

However, overall, for a wet-state interface that promises electrodes with reliable contact with hairy scalp, the challenge is to accomplish long-term reliable EEG recording for over 1-day continuous wearing of the electrodes. The simplex phase of the wet-state interface leads to the inadequate dynamic adaptability of electrodes to hairy scalp, which makes it challenging to maintain long-term stable contact of electrodes with hairy scalp. For liquid-like interface materials, their inferior cohesion would result in their

Department of Electrical Engineering and Information Systems, The University of Tokyo, 7-3-1 Hongo, Bunkyo-ku, Tokyo 113-8656, Japan.
*Corresponding author. Email: someya@ee.t.u-tokyo.ac.jp

dislocation/spreading possibility and weak mechanical interaction with electrodes (*8*). Solid-like interface materials such as conductive hydrogels have been proposed to address the limitations of liquid-like interface materials (*5*, *17*, *18*). For solid-like interfaces, dense hairs would become obstacles for them to form efficient contact with hairy scalp; thus, elaborate structure design such as claw-like and columnar structures is developed to achieve reliable contact (*17*, *18*). Furthermore, it is important that the electrode materials can be facilely removed after the designated service life without causing skin damage. Developing an engineered-material strategy that could combine all favorable attributes into one interface material, including superior cohesion, capability to form stable and effective contact with hairy scalp without additional intervention, and easy removal property, is meaningful for long-term capture of high-quality EEG signals.

Here, we developed a biocompatible on-skin paintable conductive biogel, which showed temperature-controlled reversible phase transition between the fluidic state and viscoelastic gel state, as well as water-triggered removal property to address the aforementioned challenge. We further demonstrated its promising application as highly effective and stable interface for long-term reliable EEG recording through hairy scalp, and for the high-efficiency capture and classification of steady-state visually evoked potentials (SSVEPs) (Fig. 1A). Owing to its ability of temperature-controlled phase transition between viscous fluid and viscoelastic gel, the biogel with good biocompatibility and safety can be directly painted on the skin and/or hairy scalp and then be transformed into a mechanically robust hydrogel through in situ gelatinization. These favorable merits of the biogel make it superior as reliable interface to achieve the conformal contact and dynamic compliance of electrodes with hairy scalp, which contributes to the long-term high-fidelity EEG recording over continuous wearing of electrodes for several days without the need for additional mechanical fixtures to secure the electrodes. Furthermore, the high-quality capture of SSVEPs by the biogel electrodes and the high classification accuracy achieved by a convolutional neural network (CNN)–based learning architecture were demonstrated, signifying the potential application of the biogel in SSVEP-based brain-machine interfaces (BMIs).

RESULTS

On-skin paintable biogel with temperature-controlled fluid-gel phase transition merit for long-term reliable EEG recording interface

To implement the proposed design of the on-skin paintable biogel, cost-effective and naturally derived gelatin was used as the main matrix, and other biocompatible constituents were used as functional components, including sodium chloride for ionic conductivity, sodium citrate for ionic cross-linking, and water-glycerol binary solvent system for long-term stability. Gelatin was chosen as the main matrix, as it is a well-known FDA-approved water-soluble biopolymer with good biocompatibility, biodegradability, nontoxicity, and large-scale production. In addition, gelatin shows a unique thermoreversible phase transition feature that is associated with its chain structure transformation between random coils and triple helix (*19*, *20*). Owing to its unique merits, gelatin has been studied as hydrogels for soft biodegradable electronic sensor patches or wearable strain sensors for detecting physiological signals such as temperature, humidity, and human motions (*20*, *21*). In these reference literatures, the phase transition of gelatin was used for healing, assembling, and recycling gelatin hydrogels. In this work, the phase transition feature of gelatin biogels is designed for effective and reliable interface for EEG monitoring for hairy scalp. Besides, to make it suitable for the direct usage on human skin, the transition temperature of the biogel is further adjusted by tuning the cross-link density in the biogel matrix (see details below).

In the binary solvent system, the glycerol forms more stable hydrogen bonding with water and then provides the water-locking effect in the biogel, thereby preventing the dehydration of biogel and making it relatively stable over the long term (*22*). Electrical impedance of the biogels with different glycerol content was measured to qualitatively reveal the optimization of glycerol content for low interface resistance. A trade-off between the dehydration prevention and electrical impedance of the biogel interface was observed (fig. S1). The dehydration prevention effect increased with the increase in glycerol content (fig. S1A), whereas a biogel with a much higher glycerol content showed a higher initial electrical impedance (fig. S1, C and D). A biogel with the appropriate glycerol content showed a lower electrical impedance after 24 hours (fig. S1, E and F), implying an optimized glycerol content (Biogel-Gly3/4 formulation).

An optimization of the sodium chloride content was also conducted to determine the appropriate sodium chloride content for the paintable biogel (fig. S2). Despite the lower electrical impedance induced by the higher sodium chloride content (fig. S2, A and B), the biogels with different sodium chloride showed similar skin contact impedance (fig. S2, C and D). Besides, sodium chloride crystallized out after the biogel with much higher sodium chloride content was painted and kept for 48 hours (fig. S2E), implying an optimized sodium chloride content (biogel with 2 M NaCl formulation). Biogels with the optimized glycerol and sodium chloride contents were used for further experiments and demonstration. In addition, the introduction of functional additives did not compromise the biodegradability of the biogel, as demonstrated by the microbial corrosion–induced rapid degradation of the biogel in the soil (fig. S3); thus, the biogel can be considered as environmentally benign and sustainable.

Owing to its reversible noncovalent cross-links (such as the main triple-helix junctions and ionic cross-links in the biogel matrix), the biogel could transform into a fluidic state at high temperature (Fig. 1B) and then into a solid-like gel state at room temperature (Fig. 1C), thereby demonstrating its thermally responsive reversible liquid-gel transition properties. Its good biocompatibility and nontoxicity makes the thermal liquid biogel ink capable of being directly painted on the skin surface. Then, the painted biogel ink spontaneously gelatinized into the biogel with mechanical robustness and good adhesion to the skin (Fig. 1, D and E, and movie S1). Besides, the fluidic biogel on the skin surface followed the microscopic curvature of the skin texture before its in situ gelation, leading to the conformal contact of gelatinized biogel with the corrugated skin surface, as demonstrated by the replicated microscopic skin texture structure on the surface of the peeled-off on-skin painted biogel (Fig. 1F). The fluidity of the thermal biogel ink allowed for the good conformability and conformal contact of the painted biogel with the hairy scalp with no hair interference (Fig. 1G), which is superior to preformed gels and is beneficial for high-quality EEG recording through hairy scalps.

The thermally triggered liquid transition of the biogel is also useful for its facile removal from the hairy scalp by hot water after the designated lifetime without causing skin damage (Fig. 1H). Compared

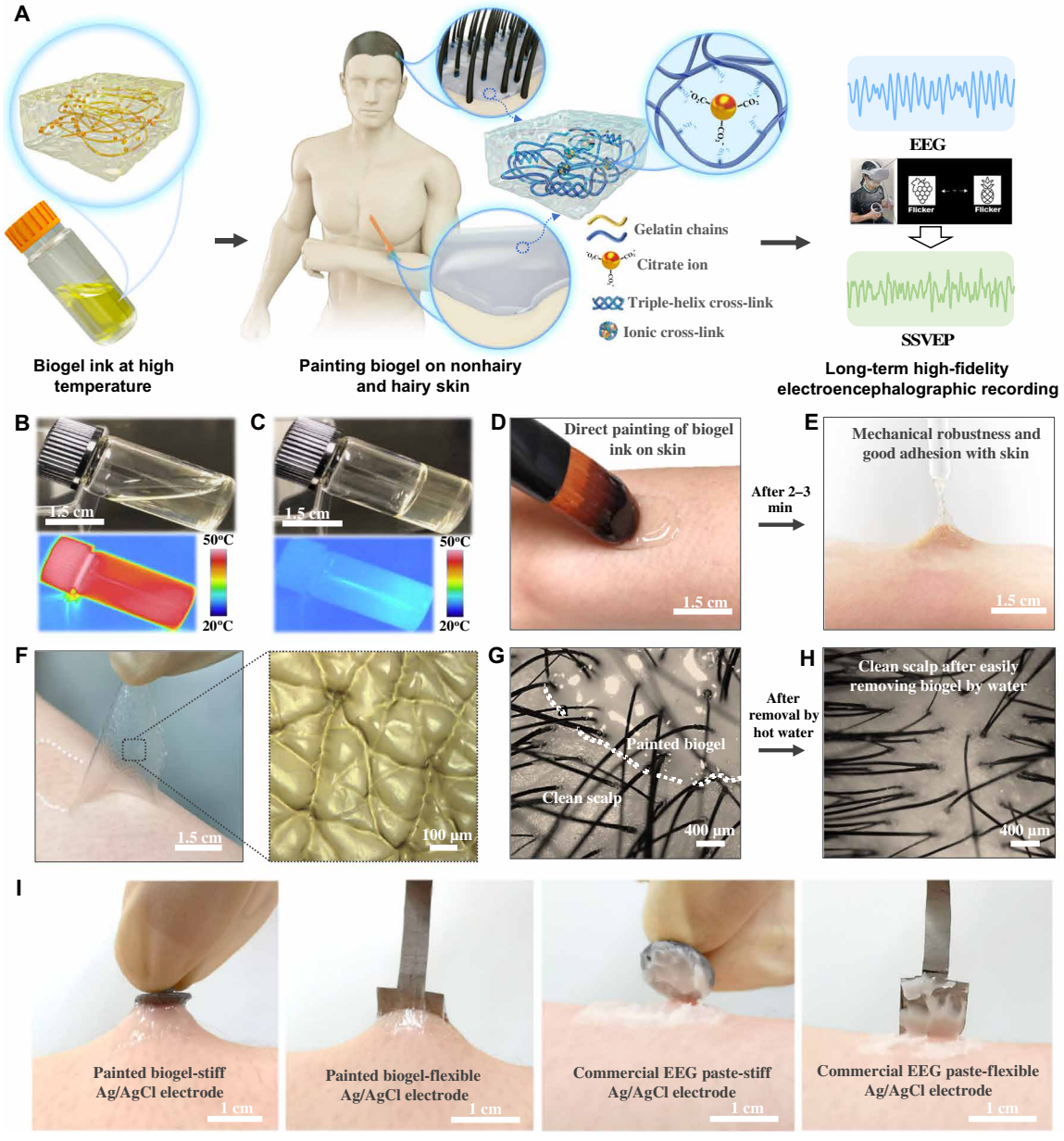

Fig. 1. On-skin paintable biogel interface for high-fidelity EEG recording. (**A**) Schematic illustration showing the concept of on-skin paintable biogel for hairy scalp for EEG recording (e.g., typical EEG signal and SSVEP). (**B** and **C**) Photographs and infrared camera images of biogel at high temperature (B) and room temperature (C), demonstrating the transition of biogel between fluidic state at high temperature and solid-like gel state at low temperature. (**D** and **E**) Photographs of direct painting biogel ink on skin (D) and in situ gelatinized adhesive biogel on skin after 2 to 3 min (E), showing its on-skin painting capability and good adhesion with skin. (**F**) Photograph and optical image of peeled-off on-skin painted biogel (upper) and the replicated skin texture structure on its surface (lower), showing its conformal contact with the corrugated skin surface. (**G** and **H**) Optical images of biogel painted on the hairy scalp (G) and clean scalp after removing biogel by water (H), showing its good contact with scalp with no hair interference and its easy removal. (**I**) Photographs showing the superior attachment of Ag/AgCl electrodes with painted biogels compared to commercial EEG paste.

to commercial EEG paste/gel with inferior internal cohesion, another advantageous merit of the biogel is its superior cohesiveness induced by in situ gelatinization, which contributes to its superior mechanical interaction with electrodes. As demonstrated in Fig. 1I and figs. S4 and S5, the painted biogel could immobilize the Ag/AgCl electrodes firmly on the skin surface without any additional physical fixation. When pulled, these electrodes were still tightly attached to the stretched skin, whereas for commercial EEG pastes and adhesive gels, the electrodes were easily detached (Fig. 1I and fig. S4). When pulling electrodes attached to the hairy scalp, the electrode kept connected to the stretched biogel, whereas electrodes were detached from commercial paste and gel (fig. S5). The superior mechanical interaction is of great benefit for EEG recording through hairy scalp with no cumbersome fixture system required to fasten the electrodes and for dynamic adaptability of electrodes with scalp.

Synthesis and characterization of the on-skin paintable biogel

The transition temperature for the biogel from viscous liquid to viscoelastic gel was adjusted to make it suitable for direct on-skin usage, as the skin temperature for different points on the human body is normally about 37°C (*23*, *24*). The physical cross-link content in the biogel matrix has influence on its phase transition temperature, because the thermal-responsive phase transition is caused by the disaggregation and aggregation of the physical cross-links in the biogel matrix at high and low temperature (*25*). A higher cross-link density in the gel matrix would result in a higher phase transition temperature. The cross-link density in the biogel matrix was adjusted by altering the gelatin molecular weight, which has positive influence on the triple-helix cross-links, and by introducing additional ionic cross-links. Compared to a biogel based on gelatin with a small molecular weight (Biogel–175-g Bloom formulation), a biogel based on gelatin with a large molecular weight (Biogel–300-g Bloom formulation) showed a higher cross-link density, as demonstrated by its lower swelling ratio (fig. S6). Besides, ionic cross-links were introduced into the biogel matrix by the addition of sodium citrate to further increase the cross-link density. Under proper conditions, the triple carboxylate groups of citrate anions could have ionic interaction with the amino groups of gelatin chains to form amine-carboxylate electrostatic domains, leading to the introduction of ionic cross-links into the gelatin networks (*21*). A biogel with sodium citrate (Biogel–300-g Bloom with Na_3Cit formulation) exhibited the lowest swelling ratio among the biogel samples (fig. S6), indicating its highest cross-linking density.

To verify the design concept of the temperature-controlled reversible viscous liquid-viscoelastic gel transition, the rheological properties of representative biogels with different recipes (Biogel–175-g Bloom, Biogel–300-g Bloom, and Biogel–300-g Bloom with Na_3Cit formulation) in response to temperature changes (cooling and heating process) were characterized and compared (Fig. 2, A and B, and fig. S7). During the cooling process, both the storage modulus G' and loss modulus G'' for all the biogels increased evidently and continuously as the temperature decreased (Fig. 2A). The corresponding tanδ (G''/G') decreased to less than one at ~23.8°, ~28.9°, and ~35.9°C for biogels based on 175-g Bloom gelatin, 300-g Bloom gelatin, and 300-g Bloom gelatin with Na_3Cit, respectively (Fig. 2B), signifying their transition temperature from viscous liquid to viscoelastic gel at those temperatures (approximately). The increasing trend of the transition temperature for these biogels is in accordance with their cross-link density trend. In addition, the liquid-gel transition temperature for the optimized biogel (300-g Bloom gelatin with Na_3Cit formulation) is suitable for direct painting and in situ gelation on the skin surface. During the heating process, the biogels showed decreased storage and loss moduli with increasing temperature, and all the tanδ values increased beyond one at above 45°C, implying reversible transition from a solid-like state to liquid-like state at high temperature (fig. S7). The temperature dependence of rheological properties of the biogels indicates that the biogel could transform between viscous liquid and viscoelastic gel reversibly, owing to the thermoinduced destruction and reconstruction of the physical interactions (*26*). The liquid-like fluidity of the biogel at high temperature is beneficial to enhancing conformability and conformal contact with both nonhairy and hairy skin when the thermal biogel ink is directly painted on the skin. The solid-like viscoelastic gel state of biogel

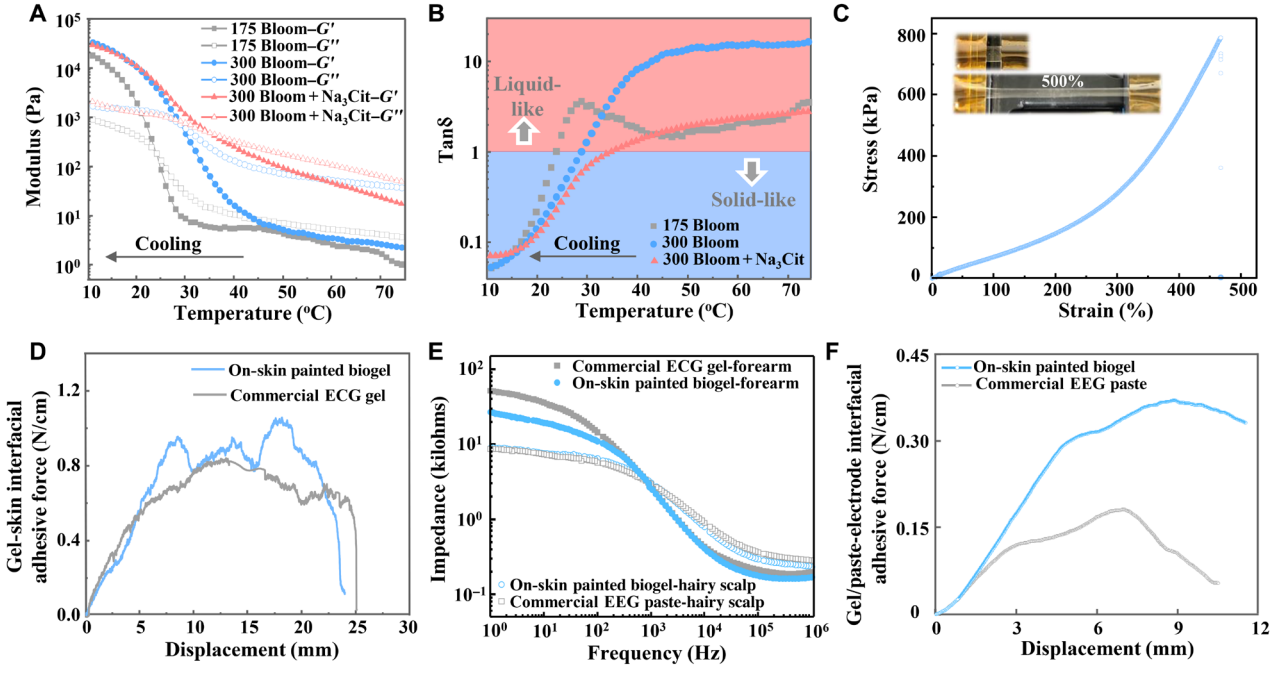

Fig. 2. Rheological, mechanical, electrical, and adhesive characteristics of on-skin paintable biogel. (**A**) Rheological characterization of biogels with different recipes at a temperature sweep from 75° to 10°C, showing their transition between viscous liquid state and elastic gel state. (**B**) The corresponding tanδ (G''/G') calculated from data in (A). (**C**) Representative stress-strain curve of biogel at ambient temperature. Inset shows the photograph of the pristine and stretched biogel at ambient temperature. (**D**) Interfacial adhesion force of on-skin painted biogel and commercial solid-like ECG gel on skin. (**E**) Electrode-skin impedance spectra for commercial solid-like ECG gel, commercial EEG paste, and on-skin painted biogels. (**F**) Adhesive force for on-skin painted biogel-electrode and commercial EEG paste-electrode interfaces.

formed on the skin through in situ gelation contributes to its superior mechanical interaction.

The optimized biogel exhibited mechanical robustness with high stretchability and tensile cyclability, which is beneficial for its practical application for conformable integration with soft and curvilinear skin surfaces. The biogel could be stretched to about five times the original length, with an average Young's modulus of 73.4 ± 2.2 kPa (five samples tested), which is lower than that of soft skin tissues (0.1 to 2 MPa) (Fig. 2C and fig. S8A), thereby favoring its good biomechanical interaction with soft skin (*27*, *28*). A successive cyclic tensile test with a maximum strain of 150% was conducted for the biogel. A small hysteresis was observed on the loading-unloading cycle, indicating its mechanical robustness and viscoelasticity (fig. S9). In addition, the adhesion performance of the on-skin painted biogel to the skin surface was evaluated by measuring the interfacial adhesive force between the painted biogel and skin through a 90° peel-off test. The on-skin painted biogel showed favorable adhesion to the skin surface compared to the commercial solid-like adhesive ECG gel (Fig. 2D), with an average adhesion force of 0.80 ± 0.076 N/cm (five biogel samples tested; fig. S8B). This can be mainly attributed to the electrostatic and van der Waals interactions between the in situ gelatinized biogel and skin surface, as induced by the amphiphilicity and chain mobility of the gelatin. The favorable interfacial adhesiveness of the painted biogel is beneficial for its good compliance with the skin in practical settings.

To obtain benign electrical communication between the electrodes and skin tissues, good coupling between the ionic flux in the skin tissue and electronic current in the electrode is essential, which could be expected by applying a compliant hydrogel with low impedance as the interface between the electrode and skin. The optimized biogel with a thickness of ~1.5 mm showed a low electrical impedance (~155 ohms at 100 Hz) in the thickness (interface) direction (fig. S10), which is favorable for a low electrode–skin interface resistance. Owing to its conformal contact and conformability with the skin, the on-skin painted biogel exhibited a slightly lower electrode–skin electrical impedance than the commercial solid-like ECG gel of the same size (Fig. 2E). The painted biogel showed an electrode-scalp impedance similar to that of the painted commercial EEG paste of the same size, with an average impedance of 6.95 ± 0.97 kilohms at 10 Hz (five samples tested) (Fig. 2E and fig. S8C). These results contribute to its promising capability for high-fidelity electrophysiological recordings.

Furthermore, compared to commercial nonsolid EEG pastes/gels with inferior cohesion, another important advantage of the on-skin paintable biogel is that its phase transition from fluid to viscoelastic gel provides its superior cohesiveness and mechanical interaction. The mechanical interaction between the gel and flexible Ag/AgCl electrode was characterized by measuring the gel-electrode interfacial adhesive force (see details of the measurement setup in the Supplementary Materials and fig. S11A). The biogel-electrode interfacial adhesive force was more than twice that of the commercial EEG paste and gel (Fig. 2F and fig. S11B), with an average adhesion force of 0.37 ± 0.01 N/cm (five samples tested; fig. S8D), signifying the superior mechanical interaction of the painted biogel. In addition, the painted biogel exhibited much higher long-term electrical stability than the commercial EEG paste and adhesive gel, as demonstrated by its much lower impedance change after 24 hours (fig. S12), which is favorable for long-term reliable EEG recording.

The combined merits of the painted biogel, including conformal contact, good compliance with soft skin, and low electrical impedance, make it promising as reliable interface for high-fidelity electrophysiological recording. The recording of ECG and EMG signals, which can be detected through nonhairy skin, was first demonstrated using painted biogel electrodes with the subject in a sedentary state and with transmission in a wireless mode (figs. S13 to S17). High-fidelity ECG signals with distinguishable PQRST waveforms and a signal-to-noise ratio (SNR) of 36.7 dB were successfully recorded by the biogel electrodes, which showed similar waveforms but superior SNR compared to ECG signals detected by commercial gel electrodes (SNR of 33.5 dB; fig. S14A). Besides, the biogel electrodes showed higher-quality ECG signals with more discriminable PQRST waveforms and higher SNR (37.8 dB) during workout-induced mild sweating (fig. S14B, top). This higher signal quality may arise from two factors: (i) When sweating, the slightly increased skin temperature would cause the slightly decreased modulus of the biogel and then the superior compliance of biogel with skin. (ii) The uptake of salt-contained sweat by the biogel may slightly improve its ionic conductivity. The superior recording performance of the painted biogel electrodes during sweating is of great benefit to electrophysiological monitoring during daily activities.

Furthermore, the painted biogel electrodes provided the long-term high-fidelity capture of ECG signals, as supported by the high-quality ECG signals (SNR of 37.6 dB) recorded after continuous wearing for 24 hours (fig. S14B, bottom). The electrode-skin impedance for the painted biogel after 24 hours of continuous wearing showed negligible changes at high frequency and a slight decrement at low frequency (fig. 15A), which is mainly attributed to the sweat secretion of the skin and sweat uptake of the biogel (*29*, *30*). Owing to its good biocompatibility, the on-skin painted biogel exhibited no adverse effects on the skin after wearing the biogel for 24 hours (fig. S15B). Wireless electrophysiological signal monitoring can provide on-site and on-time detection of health-related biopotential signals and is of great importance for point-of-care health care monitoring and diagnostic treatment (*31*). Continuous and wireless ECG signal recordings during various representative daily activities (including executing office work, walking, and jogging) were obtained by two painted biogel electrodes integrated with a commercial wireless module. They exhibited distinguishable informative subwaves and long-term stability, signifying the potential application of the biogel for wireless electrophysiological recording in daily life (fig. S16). Similar to ECG recordings, EMG signals, which can be used for determining the muscle fatigue and for application in human-machine interfaces (*32*), could also be recorded with high quality by the painted biogel electrodes, as demonstrated in fig. S17.

High-fidelity and long-term EEG recording by on-skin painted biogel electrodes

High-quality EEG recording is important for clinical and research-based neurological applications such as neurological disorder diagnoses and BMIs, as EEG recording provides an effective and noninvasive approach to monitoring brain electrical activity with fine temporal resolution (*14*, *33*). Compared to ECG and EMG signals, which can be easily detected through nonhairy skin, highly effective recording of EEG signals is much more challenging because of the weak signal (with amplitude in the microvolt range) and interference from dense hairs on the hairy scalp. Owing to its thermal-controlled liquid-gel transition and the fluidity of thermal

biogel ink, the painted biogel has good conformability and compliance with hairy scalp with no hair interference, contributing to its potential for high-quality EEG recording. As a proof of concept, EEG alpha activity from the occipital position of a hairy head was recorded by the painted biogel electrodes (see experimental details, experimental setup illustration, and the electrode position on the hairy scalp in Materials and Methods and fig. S18). The painted biogel electrode showed high-fidelity EEG alpha rhythm recording with no considerable difference from signals recorded by the commercial EEG paste during the same signal acquisition period in terms of signal shape, signal amplitude, and power spectral density (PSD) (Fig. 3, A and B). The PSD analysis (PSDA) based on EEG alpha signals recorded by both electrodes revealed a clear central peak at 10 Hz, a characteristic of EEG alpha rhythms (Fig. 3B) (*34*).

EEG signals in the eyes-open and then eyes-closed states were further recorded by the painted biogel electrode, which presented distinct differences between the signals detected in the eyes-open and eyes-closed paradigms (Fig. 3C, top). The PSDA and corresponding spectrogram showed no alpha rhythm under the eyes-open state and a pronounced alpha rhythm in the eyes-closed state [Fig. 3C (bottom) and fig. S19, A and B]. As a comparison, EEG signal recording performed by a commercial EEG paste electrode in the eyes-open/eyes-closed paradigms matched well with those captured by the biogel electrode (fig. S19, C to E). In addition, high-quality EEG alpha rhythm recordings in both the eyes-closed and eyes-open/eyes-closed paradigms were successfully conducted by biogels with smaller sizes (diameters of ~6 and ~4 mm), and these also showed evident alpha characteristic peaks in their PSDA (fig. S20). The capability of recording high-quality EEG signals with small-sized biogel electrodes provides a promising possibility for implementing high-density EEG configurations for capturing neural information with high spatial resolution (*35*).

Owing to its compliance with the hairy scalp, stable attachment with flexible electrodes, and long-term electrical stability, the painted biogel was demonstrated with the remarkable capability for long-term EEG recording with high quality. EEG alpha signals recorded by the biogel electrode for more than 8 min exhibited stable rhythmic and periodic patterns throughout the entire signal, as demonstrated by the zoomed-in alpha rhythms with characteristic peaks of 10 Hz in their PSD (Fig. 3D). The PSDA of the overall alpha signals showed a clear alpha rhythm characteristic (fig. S21). Besides, long-term EEG recording was performed over several hours (see the schematic illustration of the experimental setup in fig. S22A), from which the biogel showed superior recording stability compared to commercial EEG adhesive gel. Figure 3E presents the declined power ratios of the EEG alpha signals recorded by the commercial gel and the biogel electrodes after several hours, implying the signal degradation for the commercial gel. The signal power was calculated on the basis of the PSDA of the EEG alpha rhythms (8 to 12 Hz). The EEG signals and PSDA revealed inferior signal quality with relatively lower alpha rhythm feature peaks for commercial gel electrodes after 3 and 5 hours relative to the biogel electrode (Fig. 3, F and G, and fig. S23).

Furthermore, the painted biogel allowed for the long-term high-fidelity capture of EEG signals for over 1 day of continuous wearing of electrodes, owing to its relatively long-term electrical stability, superior mechanical interaction, and stable contact with the scalp. For commercial EEG pastes/gels, it is inappropriate for EEG recording over 1-day continuous wearing of electrodes because of the easy electrode detachment caused by their nonsolid state and the fast electrical degradation induced by their dry-out susceptibility. Semidry electrodes with an electrolyte solution reservoir and dry contact electrodes have been developed as possible techniques for implementing long-term recording, yet cumbersome mechanical fixture and elaborate structure design are generally needed to achieve contact with hairy scalp, and they usually showed relatively inferior signal quality to wet electrodes (*6*, *14*, *36*). As for another kind of dry electrodes with ultrathin film structure, they are only suitable for nonhairy skin location for EEG detection (*11*, *16*). The informative comparison between the painted biogel and other electrodes for long-term EEG detection is illustrated in table S2.

EEG alpha rhythms were collected by the biogel with a flexible Ag/AgCl electrode after continuous wearing for 24, 48, and 72 hours to verify the superior long-term high-fidelity EEG recording ability of the painted biogel. Every time the long-term recording was performed by the biogel electrode, a conventional standard electrode with commercial EEG paste was freshly applied nearby to simultaneously detect EEG alpha signals for comparison (see the schematic illustration of the experimental setup in fig. S22B). All the EEG alpha signals recorded after different wearing durations of the biogel electrode (0, 24, 48, and 72 hours) showed no notable difference and high quality with distinct periodic patterns with peak frequency at 10 Hz (Fig. 3H). Besides, the long-term EEG alpha rhythms captured by the biogel electrode were nearly identical to the signals detected by the contradistinctive freshly applied conventional EEG paste electrodes (fig. S24), signifying the promising capability of the painted biogel for long-term high-fidelity EEG recording. Note that gas permeability for on-skin biogels is important for much longer-term application. For now, the as-developed on-skin paintable biogel showed inferior gas permeability because of its intact hydrogel structure. The developing of biogels with good gas permeability by material engineering and structure design would be focused on in the future.

High-accuracy classification of SSVEPs by using on-skin painted biogel electrodes

The high-fidelity recording capability of the painted biogel for EEG signals is in favor of its potential application in EEG-based BMIs. The SSVEP has attracted more attention as a promising EEG source for BMIs, as SSVEP-based BMIs could provide high information throughput, minimal user training requirements, and high reliability (*14*). The capture and classification of SSVEPs is of great importance for SSVEP-based BMIs. First, the SSVEP recording by the biogel electrode was conducted with white light-emitting diode (LED) stimulation as the flicker to demonstrate its SSVEP capture capability (see the Supplementary Materials and figs. S25 and S26). All the recorded SSVEPs exhibited prominent peaks corresponding to the stimulation frequencies in their PSDA (figs. S27 to S30), implying that frequency-dependent brain activity could be elicited by LED stimuli (*37*). Besides, the classification of SSVEPs evoked by arrays of stimuli is important for BMIs, e.g., to provide control over different targets (*14*). The SSVEP-based spatial attention classification was carried out on the basis of the capture of SSVEPs by the biogel electrode, and a head-mounted display (HMD) was used to present two flickers with different frequencies in a virtual reality (VR) environment to evoke SSVEPs (Fig. 4A). This conceptually demonstrated the potential of using the biogel as an effective interface for the BMI-VR system.

The time-domain SSVEP data with a 3-s segment and their PSDA proved that SSVEPs with a characteristic frequency could be evoked

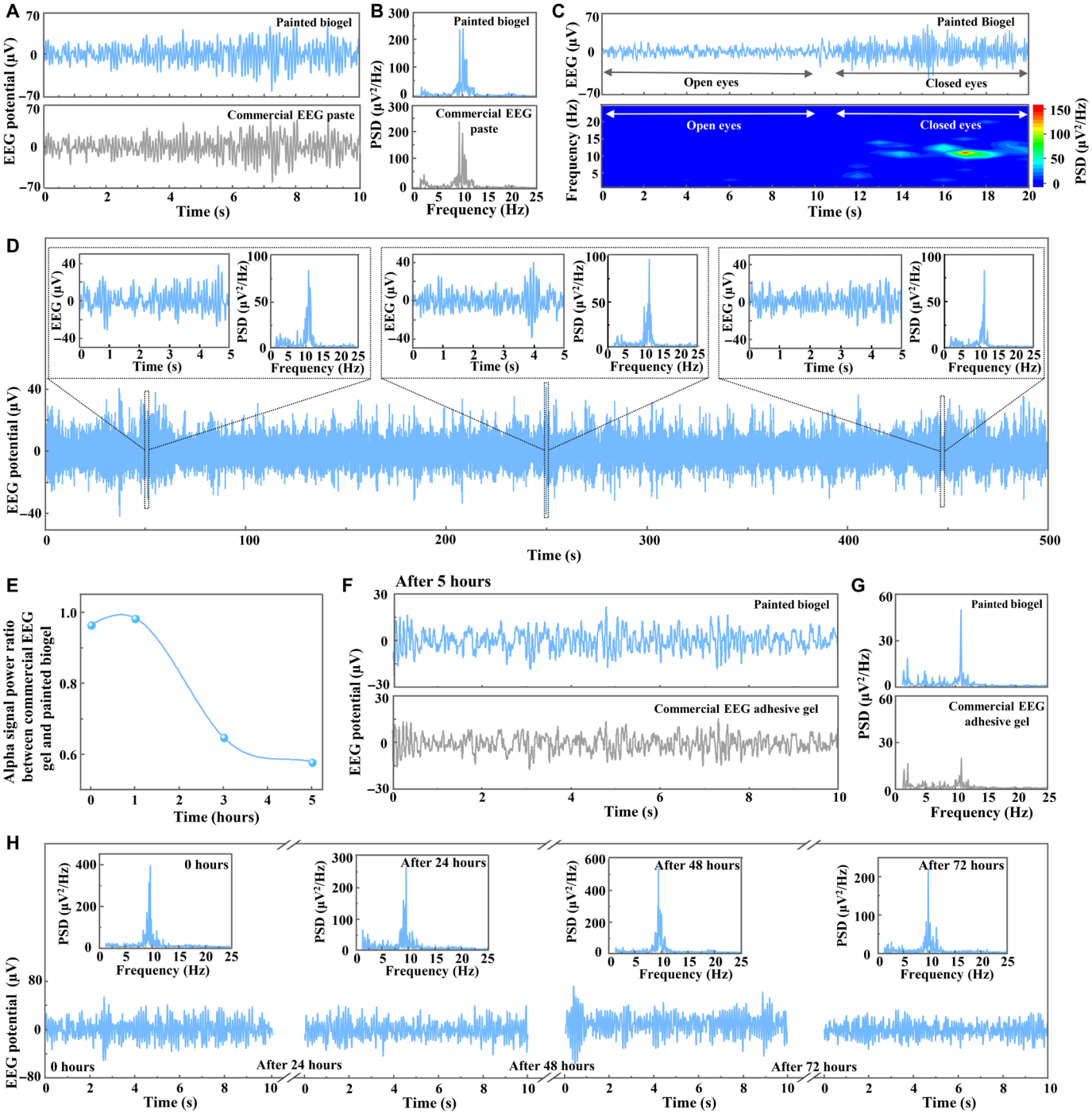

Fig. 3. High-fidelity and long-term EEG recording for hairy scalp by on-skin painted biogel electrodes. (**A**) EEG alpha rhythms recorded by the painted biogel (top) and commercial EEG paste (bottom). (**B**) PSDA for EEG signals in (A). (**C**) EEG signals recorded by the painted biogel in the eyes-open/closed paradigm (top) and the corresponding spectrogram showing clear alpha rhythm in the eyes-closed state (bottom). (**D**) Long-period EEG alpha rhythms continuously recorded by the painted biogel electrode. Insets show the zoomed-in data segments and their PSDA. (**E**) Power ratio of EEG alpha signals recorded by the painted biogel electrode and commercial EEG adhesive gel electrode over a duration of several hours. (**F** and **G**) EEG signals recorded by the painted biogel and commercial adhesive EEG gel electrodes after 5 hours (F) and their PSDA (G). (**H**) EEG alpha rhythms recorded by the painted biogel electrode after continuous wearing for 0, 24, 48, and 72 hours. Insets show their PSDA.

when the subject concentrated on the flicker with the same frequency (Fig. 4, B and C), which is important for high classification accuracy of SSVEP-based attention. To further quantify the classification accuracy, we used a seven-layer CNN for the analysis (see details in Materials and Methods and fig. S31). A slightly individual-dependent high classification accuracy of SSVEPs was achieved with an average accuracy of 97.17% (time length: 3 s) based on this CNN analysis (Fig. 4D). The average classification accuracy for different time lengths

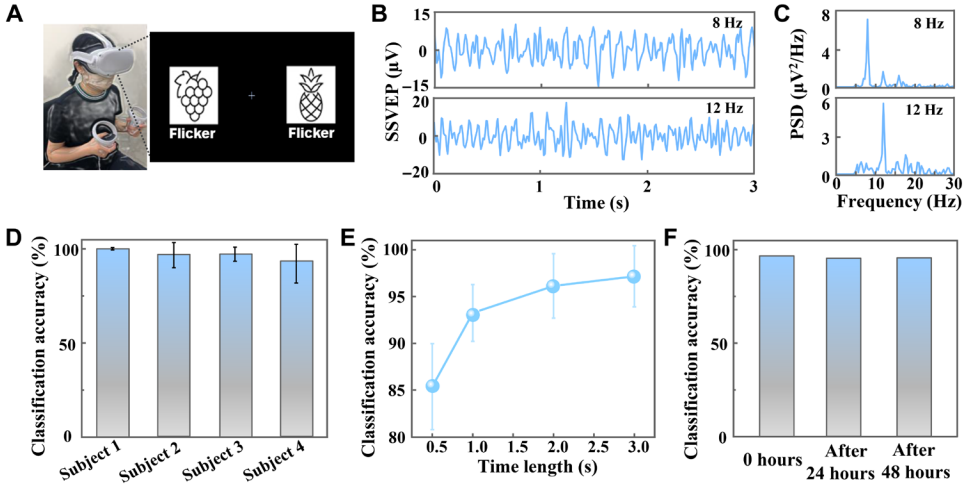

Fig. 4. Classification of SSVEPs recorded by the on-skin painted biogel electrodes. (**A**) Dual visual field stimulus paradigm by a VR HMD, in which the left character flickered at 8 Hz and the right character flickered at 12 Hz. (**B**) SSVEP signals recorded when the subject gazed at 8-Hz flicker (top) and 12-Hz flicker (bottom) in a VR environment. (**C**) PSDA for SSVEP signals in (B). (**D**) SSVEP classification accuracy for different subjects. (**E**) SSVEP classification accuracy with different time scales. (**F**) SSVEP classification accuracy after different long-term duration.

revealed that larger time lengths would result in higher classification accuracies, to be specific, 93.24% for 1 s, 96.14% for 2 s, and 97.17% for 3 s (Fig. 4E). Furthermore, the classification accuracy of SSVEPs captured by the biogel electrode after different continuous wearing (0, 24, and 48 hours) showed insignificant difference (Fig. 4F), which demonstrated the capability of the biogel as reliable interface for SSVEP-based applications for long-term duration. The effective capture and high classification accuracy of SSVEPs even after long-term duration make it a potential and promising effective interface for BMIs.

DISCUSSION

In summary, we introduced a biocompatible on-skin paintable conductive biogel for long-term high-fidelity electrophysiological recording and notably for high-performance EEG recording through the hairy scalp. This biogel shows the unique merit of temperature-controlled reversible phase transition between viscous fluid and viscoelastic gel, thereby endowing it with the prominent capability in regard to the on-skin paintability and in situ gelatinization, which contributes to the conformal contact and dynamic compliance of electrodes with the hairy scalp. The biogel was demonstrated as highly effective and reliable interfaces for the high-fidelity capture of EEG signals and SSVEPs, even after continuous wearing of the biogel electrode for several days. Highly accurate classification of SSVEPs recorded in a VR environment was obtained using a CNN-based algorithm. The on-skin paintable biogel offers a promising engineered-material strategy to achieve biocompatible, reliable, and stable interfaces for advanced EEG recording systems and EEG-based BMIs.

MATERIALS AND METHODS

Materials and preparation of on-skin paintable biogel

All chemicals were purchased from Sigma-Aldrich, including type A gelatin powders (isoelectric point of 7.0 to 9.5) with different Bloom numbers (~175-g Bloom and 300-g Bloom), sodium chloride, sodium citrate, citric acid, and glycerol. For biogels based only on physical cross-linking between gelatin chains, sodium chloride (0.46 g) was dissolved in deionized water (4 ml), followed by adding and mixing glycerol (3 g), and then gelatin powder (2 g) was introduced into the solution and soaked for 2 hours. The mixture was then kept in an oven at 75°C for 45 min to dissolve the gelatin well, and a planetary mixer was used to achieve a homogeneous gelatin solution that would transform into a gel after the temperature cooled down. Biogel recipes with other compositions are listed in table S1. For biogels based on physical cross-linking between gelatin chains, and ionic cross-linking between gelatin chains and citrate ions, the same procedure was conducted, with the exception of dissolving citric acid (0.05 g) and sodium citrate (0.5 g) simultaneously with sodium chloride. The role of citric acid was to adjust the pH of the solution to 6 to 7, resulting in ionic interactions between the gelatin chains and citrate ions. Next time before usage, the biogel was reheated to 60° to 75°C for several minutes to transform it into a liquid state, which was then directly painted on nonhairy skin and hairy scalp for electrophysiological recording. No thermal damage to skin was observed for all subjects. Generally, the fluidic biogel painted on the skin would spontaneously transform into a viscoelastic gel after several minutes, and cool air blowing by a hair dryer can be used to further reduce the transformation time.

Characterization of rheology, adhesiveness, mechanical property, and impedance

The rheological testing was performed in modes of dynamic temperature sweep with a rheometer. The temperature sweep was conducted from 10° to 75°C and then from 75° to 0°C at a rate of 2°C/min, an oscillation frequency of 2π rad/s, and a gradually increased shear strain amplitude from 0.08 to 10%. The interfacial adhesiveness of the skin or flexible Ag/AgCl electrode with the on-skin painted biogel was measured in comparison with the commercial preformed solid-like adhesive gel (Vitrode F, NIHON KOHDEN) and commercial EEG paste/gel (Elefix paste for EEG, NIHON KOHDEN, and TENSIVE conductive adhesive gel). All adhesiveness measurements were performed through a 90° peeling process using a stretcher (AG-X, Shimadzu, Japan) with a perpendicular delamination rate

of 50 mm/min. The single and cyclic tensile measurements were conducted using an AG-X stretcher with tensile speed rates of 10 and 45 mm/min, respectively. To measure the electrical impedance of the biogels with different glycerol and sodium chloride content, biogels were painted on the patterned Au electrodes and a cuboid-shaped mold (1 cm by 2 cm by 1.0 mm) was used to control the shape of the painted biogels (fig. S1B). To measure the electrical impedance of the biogel interface in the thickness direction, biogels with a thickness of ~1.5 mm were sandwiched between top and bottom Au-deposited polyimide sheet electrodes (fig. S10A). An LCR meter (E4980AL, Keysight) was used to record the impedance. The skin contact impedance was recorded using an LCR meter (ZM2376, NF) and a two-electrode system with the painted biogels, commercial ECG solid gel, or commercial EEG paste as the interface between the Ag/AgCl electrodes and forearm/hairy scalp. The distance between two electrode adjacent edges was ~1.5 cm. The biogels were painted on the skin with the same size as the commercial ECG gels (2.0 cm by 2.5 cm) and commercial EEG paste (diameter: ~10 mm). All impedance measurements were conducted at an amplitude of 100 mV.

Electrophysiological recording through nonhairy skin and hairy scalp

The ECG and EMG signals were recorded using the painted biogel electrodes to demonstrate their applications in electrophysiological recording through nonhairy skin. For the ECG recording in a sedentary state, two biogel films were painted on the left inner wrist and right inner ankle with flexible Ag/AgCl electrodes as the recording electrodes, and the same type of electrode was placed on the other inner ankle as the ground electrode. The electrodes were connected to a signal-recording equipment (Neuropack S1, NIHON KOHDEN), which recorded and processed signals with a band-pass filter (0.02 to 50 Hz). The experimental setup for the ECG recording is shown in fig. S13. For the wireless ECG recording, two painted biogels with Ag/AgCl electrodes were placed on the chest and integrated with a commercial wireless module with recording, processing, and transmission circuits, and the corresponding PC software was used to record the signals. The EMG recording for signals generated by the brachioradialis muscle was conducted by painting two biogel electrodes on the forearm and another biogel electrode on the hand dorsum as the ground electrode. The signal-recording equipment (Neuropack S1, NIHON KOHDEN) recorded and processed the EMG signals with a band-pass filter (10 Hz to 10 kHz). The experimental setup for the EMG recording is shown in fig. S17 (A to C).

Two healthy male and female subjects with dense scalp hairs (32 years old for the male subject and 31 years old for the female subject) participated in the EEG recordings. Biogels with different diameters (~10, ~6, and ~4 mm) were painted on the hairy scalp at the occipital position of the head according to the 10-20 international electrode placement system, and the flexible Ag/AgCl electrodes were integrated with the painted biogel and connected to a dual-channel bioelectric amplifier (MEG-5200, NIHON KOHDEN) for recording and processing the EEG signals with a band-pass filter (generally 1.5 to 30 Hz, but 1.5 to 100 Hz for LED stimulation with a frequency of 36 and 48 Hz). If not specified, the diameter of the painted biogels for EEG recordings was ~10 mm. In comparison, the commercial EEG paste with a standard silver disk electrode (diameter: ~10 mm) was positioned adjacent to the painted biogel electrode with a center-to-center distance of ~1.5 cm, which is reasonable for a relatively fair comparison in view of the negligible effect of their location on the EEG signals. To assess the EEG signal quality, dual-channel signals were simultaneously recorded by the painted biogel electrode and commercial paste electrode using a bioelectric amplifier with the same reference and ground electrodes on the ears. The EEG recording setup illustration and photographs indicating the positions of the electrodes on the head are shown in fig. S18. The EEG signals were generated with the subjects closing their eyes in a relaxed state and with the subjects opening then closing their eyes in a relaxed state, and were recorded to demonstrate the high-quality EEG recording of the painted biogel electrodes.

For the long-term recording (several hours) experiments, the EEG alpha signals were recorded by the painted biogel electrode placed at the occipital position and simultaneously by the commercial adhesive EEG gel electrode placed adjacent to the biogel electrode, after different numbers of hours (1, 3, and 5 hours). For the long-term recording (over 1 day) experiments, the EEG alpha rhythms were recorded by the painted biogel electrode, which was positioned at the occipital area with no protective coating after continuous wearing for different duration (24, 48, and 72 hours). For comparison, a commercial EEG paste electrode was freshly placed near the painted biogel electrode every time long-term EEG recording was conducted by the painted biogel electrode after the different wearing durations. An illustration of the long-term EEG recording setup is shown in fig. S22.

For the recording of the SSVEPs, two different types of flickers, namely, LED and VR HMD, were used for the generation of visual stimuli. For the SSVEP recording based on LED flickers, white LED stimulation with different light intensities and frequencies was driven by a function/arbitrary waveform generator (33220A, Agilent), and the painted biogel electrode was placed on the occipital lobe position (O_z) to capture the SSVEP signals. The experimental setup for the SSVEP recording under LED stimulation is shown in fig. S25. A left-right visual field stimulus paradigm with two flickering characters of different frequencies (8 and 12 Hz for left and right characters, respectively) was presented by a VR HMD (Oculus, Facebook) to evoke the SSVEPs captured by a painted biogel electrode placed in the O_z position, which was designed for the SSVEP-based spatial attention study. Four healthy volunteers aged 21 to 31 years were included in this study. The SSVEP data were collected by a continuous EEG recording for 12 s of gazing at one of two characters with equal probability; this was regarded as a single trial. Twenty trials were performed for each subject to gather SSVEP data to evaluate the classification accuracy. All experiments for this project were thoroughly reviewed and approved by the ethical committee of The University of Tokyo (approval number KE20-112), and informed consent was obtained from all subjects participating in the on-skin experiments.

Analysis of electrophysiological signals and SSVEP-based spatial attention classification

The raw ECG signal data captured in a sedentary state were processed by band-pass filtering with cutoff frequencies of 0.5 and 50 Hz, and then were plotted versus time. The raw ECG signal data captured wirelessly and the raw EMG signal data were plotted versus time without further processing. For the ECG data, the SNR values were calculated on the basis of the peak-to-peak voltage of the signal and SD of the noise voltage (*38*). The raw EEG data were further processed by band-pass filtering with cutoff frequencies of 1.5 and 30 Hz, and the raw SSVEP data recorded under the LED stimulation

with frequencies of 36 and 48 Hz were processed by band-pass filtering with cutoff frequencies of 1.5 and 50 Hz. For the PSDA, the discrete Fourier transform was conducted on the processed EEG data using MATLAB.

Preprocessing was performed on the raw SSVEP data recorded under the left-right visual field stimulus by a VR HMD, including 5- to 30-Hz band-pass filtering and segmentation of the data. To enable short-time classification and capture hidden features undetectable by simple filtering, a seven-layer CNN model, which contains five one-dimensional convolutional layers followed by two fully connected layers, was built for the SSVEP classification. The samples fed to the CNN model were obtained from each SSVEP trial data with different time windows of 0.5, 1, 2, and 3 s (corresponding to data points of 50, 100, 200, and 300 based on the sampling rate of 100 Hz) to evaluate the accuracy changes over different time scales, and with the time window shifted by 0.1 s (see fig. S32). The input to the CNN model was one-dimensional time sequence data with lengths of 50, 100, 200, or 300 data points. To calculate the classification accuracy, a fivefold cross-validation was conducted for the samples obtained from each subject, and samples from one trial were confirmed to be all put into one fold to prevent any data overlapping between the training and testing sets. Notably, for the evaluation of the classification accuracy for long-term durations, the SSVEP data captured at 0 hours was conducted with fivefold cross-validation to obtain the average accuracy for 0 hours, and then the optimized model was used for the classification of SSVEPs captured after 24 and 48 hours.

SUPPLEMENTARY MATERIALS

Supplementary material for this article is available at https://science.org/doi/10.1126/sciadv.abo1396

REFERENCES AND NOTES

1. G. Buzsáki, C. A. Anastassiou, C. Koch, The origin of extracellular fields and currents—EEG, ECoG, LFP and spikes. *Nat. Rev. Neurosci.* **13**, 407–420 (2012).
2. T. Someya, M. Amagai, Toward a new generation of smart skins. *Nat. Biotechnol.* **37**, 382–388 (2019).
3. C. Wang, K. Xia, H. Wang, X. Liang, Z. Yin, Y. Zhang, Advanced carbon for flexible and wearable electronics. *Adv. Mater.* **31**, 1801072 (2019).
4. D. Gao, K. Parida, P. S. Lee, Emerging soft conductors for bioelectronic interfaces. *Adv. Funct. Mater.* **30**, 1907184 (2020).
5. G. Li, S. Wang, M. Li, Y. Y. Duan, Towards real-life EEG applications: Novel superporous hydrogel-based semi-dry EEG electrodes enabling automatically 'charge–discharge' electrolyte. *J. Neural Eng.* **18**, 046016 (2021).
6. G.-L. Li, J.-T. Wu, Y.-H. Xia, Q.-G. He, H.-G. Jin, Review of semi-dry electrodes for EEG recording. *J. Neural Eng.* **17**, 051004 (2020).
7. N. A. Alba, R. J. Sclabassi, M. Sun, X. T. Cui, Novel hydrogel-based preparation-free EEG electrode. *IEEE Trans. Neural Syst. Rehabil. Eng.* **18**, 415–423 (2010).
8. P. Pedrosa, P. Fiedler, L. Schinaia, B. Vasconcelos, A. C. Martins, M. H. Amaral, S. Comani, J. Haueisen, C. Fonseca, Alginate-based hydrogels as an alternative to electrolytic gels for rapid EEG monitoring and easy cleaning procedures. *Sensor. Actuat. B Chem.* **247**, 273–283 (2017).
9. H. Yuk, B. Lu, X. Zhao, Hydrogel bioelectronics. *Chem. Soc. Rev.* **48**, 1642–1667 (2019).
10. Y.-J. Huang, C.-Y. Wu, A. M.-K. Wong, B.-S. Lin, Novel active comb-shaped dry electrode for EEG measurement in hairy site. *IEEE Trans. Biomed. Eng.* **62**, 256–263 (2014).
11. J. J. Norton, D. S. Lee, J. W. Lee, W. Lee, O. Kwon, P. Won, S.-Y. Jung, H. Cheng, J.-W. Jeong, A. Akce, S. Umunna, I. Na, Y. H. Kwon, X.-Q. Wang, Z. J. Liu, U. Paik, Y. Huang, T. Bretl, W.-H. Yeo, J. A. Rogers, Soft, curved electrode systems capable of integration on the auricle as a persistent brain–computer interface. *Proc. Natl. Acad. Sci. U.S.A.* **112**, 3920–3925 (2015).
12. J.-Y. Kim, Y. J. Yun, J. Jeong, C.-Y. Kim, K.-R. Müller, S.-W. Lee, Leaf-inspired homeostatic cellulose biosensors. *Sci. Adv.* **7**, eabe7432 (2021).
13. S. Lin, J. Liu, W. Li, D. Wang, Y. Huang, C. Jia, Z. Li, M. Murtaza, H. Wang, J. Song, Z. Liu, K. Huang, D. Zu, M. Lei, B. Hong, H. Wu, A flexible, robust, and gel-free electroencephalogram electrode for noninvasive brain-computer interfaces. *Nano Lett.* **19**, 6853–6861 (2019).
14. M. Mahmood, D. Mzurikwao, Y.-S. Kim, Y. Lee, S. Mishra, R. Herbert, A. Duarte, C. S. Ang, W.-H. Yeo, Fully portable and wireless universal brain–machine interfaces enabled by flexible scalp electronics and deep learning algorithm. *Nat. Mach. Intell.* **1**, 412–422 (2019).
15. P. Won, J. J. Park, T. Lee, I. Ha, S. Han, M. Choi, J. Lee, S. Hong, K.-J. Cho, S. H. Ko, Stretchable and transparent kirigami conductor of nanowire percolation network for electronic skin applications. *Nano Lett.* **19**, 6087–6096 (2019).
16. L. Tian, B. Zimmerman, A. Akhtar, K. J. Yu, M. Moore, J. Wu, R. J. Larsen, J. W. Lee, J. Li, Y. Liu, B. Metzger, S. Qu, X. Guo, K. E. Mathewson, J. A. Fan, J. Cornman, M. Fatina, Z. Xie, Y. Ma, J. Zhang, Y. Zhang, F. Dolcos, M. Fabiani, G. Gratton, T. Bretl, L. J. Hargrove, P. V. Braun, Y. Huang, J. A. Rogers, Large-area MRI-compatible epidermal electronic interfaces for prosthetic control and cognitive monitoring. *Nat. Biomed. Eng.* **3**, 194–205 (2019).
17. G. Shen, K. Gao, N. Zhao, Z. Yi, C. Jiang, B. Yang, J. Liu, A novel flexible hydrogel electrode with a strong moisturizing ability for long-term EEG recording. *J. Neural Eng.* **18**, 066047 (2021).
18. X. Sheng, Z. Qin, H. Xu, X. Shu, G. Gu, X. Zhu, Soft ionic-hydrogel electrodes for electroencephalography signal recording. *Sci. China Technol. Sci.* **64**, 273–282 (2021).
19. C. Wang, T. Yokota, T. Someya, Natural biopolymer-based biocompatible conductors for stretchable bioelectronics. *Chem. Rev.* **121**, 2109–2146 (2021).
20. M. Baumgartner, F. Hartmann, M. Drack, D. Preninger, D. Wirthl, R. Gerstmayr, L. Lehner, G. Mao, R. Pruckner, S. Demchyshyn, L. Reiter, M. Strobel, T. Stockinger, D. Schiller, S. Kimeswenger, F. Greibich, G. Buchberger, E. Bradt, S. Hild, S. Bauer, M. Kaltenbrunner, Resilient yet entirely degradable gelatin-based biogels for soft robots and electronics. *Nat. Mater.* **19**, 1102–1109 (2020).
21. Z. Qin, X. Sun, H. Zhang, Q. Yu, X. Wang, S. He, F. Yao, J. Li, A transparent, ultrastretchable and fully recyclable gelatin organohydrogel based electronic sensor with broad operating temperature. *J. Mater. Chem. A* **8**, 4447–4456 (2020).
22. L. Han, K. Liu, M. Wang, K. Wang, L. Fang, H. Chen, J. Zhou, X. Lu, Mussel-inspired adhesive and conductive hydrogel with long-lasting moisture and extreme temperature tolerance. *Adv. Funct. Mater.* **28**, 1704195 (2018).
23. C. Childs, Body temperature and clinical thermometry. *Handb. Clin. Neurol.* **157**, 467–482 (2018).
24. F. Suarez, A. Nozariasbmarz, D. Vashaee, M. C. Öztürk, Designing thermoelectric generators for self-powered wearable electronics. *Energ. Environ. Sci.* **9**, 2099–2113 (2016).
25. Y. Mosleh, W. de Zeeuw, M. Nijemeisland, J. C. Bijleveld, P. van Duin, J. A. Poulis, The structure–property correlations in dry gelatin adhesive films. *Adv. Eng. Mater.* **23**, 2000716 (2021).
26. S. Yang, Y. Zhang, T. Wang, W. Sun, Z. Tong, Ultrafast and programmable shape memory hydrogel of gelatin soaked in tannic acid solution. *ACS Appl. Mater. Interfaces* **12**, 46701–46709 (2020).
27. J.-H. Kim, S.-R. Kim, H.-J. Kil, Y.-C. Kim, J.-W. Park, Highly conformable, transparent electrodes for epidermal electronics. *Nano Lett.* **18**, 4531–4540 (2018).
28. L. Pan, P. Cai, L. Mei, Y. Cheng, Y. Zeng, M. Wang, T. Wang, Y. Jiang, B. Ji, D. Li, X. Chen, A compliant ionic adhesive electrode with ultralow bioelectronic impedance. *Adv. Mater.* **32**, 2003723 (2020).
29. L. Kalevo, T. Miettinen, A. Leino, S. Kainulainen, H. Korkalainen, K. Myllymaa, J. Töyräs, T. Leppänen, T. Laitinen, S. Myllymaa, Effect of sweating on electrode-skin contact impedances and artifacts in EEG recordings with various screen-printed Ag/AgCl electrodes. *IEEE Access* **8**, 50934–50943 (2020).
30. H. Y. Y. Nyein, M. Bariya, B. Tran, C. H. Ahn, B. J. Brown, W. Ji, N. Davis, A. Javey, A wearable patch for continuous analysis of thermoregulatory sweat at rest. *Nat. Commun.* **12**, 1823 (2021).
31. F. Ershad, A. Thukral, J. Yue, P. Comeaux, Y. Lu, H. Shim, K. Sim, N.-I. Kim, Z. Rao, R. Guevara, L. Contreras, F. Pan, Y. Zhang, Y.-S. Guan, P. Yang, X. Wang, P. Wang, X. Wu, C. Yu, Ultra-conformal drawn-on-skin electronics for multifunctional motion artifact-free sensing and point-of-care treatment. *Nat. Commun.* **11**, 3823 (2020).
32. L. Zhang, K. S. Kumar, H. He, C. J. Cai, X. He, H. Gao, S. Yue, C. Li, R. C.-S. Seet, H. Ren, J. Ouyang, Fully organic compliant dry electrodes self-adhesive to skin for long-term motion-robust epidermal biopotential monitoring. *Nat. Commun.* **11**, 4683 (2020).
33. A. J. Casson, D. C. Yates, S. J. Smith, J. S. Duncan, E. Rodriguez-Villegas, Wearable electroencephalography. *IEEE Eng. Med. Biol. Mag.* **29**, 44–56 (2010).
34. C. Babiloni, C. Del Percio, L. Arendt-Nielsen, A. Soricelli, G. L. Romani, P. M. Rossini, P. Capotosto, Cortical EEG alpha rhythms reflect task-specific somatosensory and motor interactions in humans. *Clin. Neurophysiol.* **125**, 1936–1945 (2014).
35. A. K. Robinson, P. Venkatesh, M. J. Boring, M. J. Tarr, P. Grover, M. Behrmann, Very high density EEG elucidates spatiotemporal aspects of early visual processing. *Sci. Rep.* **7**, 16248 (2017).

36. S. M. Lee, J. H. Kim, H. J. Byeon, Y. Y. Choi, K. S. Park, S.-H. Lee, A capacitive, biocompatible and adhesive electrode for long-term and cap-free monitoring of EEG signals. *J. Neural Eng.* **10**, 036006 (2013).
37. C. S. Herrmann, Human EEG responses to 1–100 Hz flicker: Resonance phenomena in visual cortex and their potential correlation to cognitive phenomena. *Exp. Brain Res.* **137**, 346–353 (2001).
38. S. Park, S. W. Heo, W. Lee, D. Inoue, Z. Jiang, K. Yu, H. Jinno, D. Hashizume, M. Sekino, T. Yokota, K. Fukuda, K. Tajima, T. Someya, Self-powered ultra-flexible electronics via nano-grating-patterned organic photovoltaics. *Nature* **561**, 516–521 (2018).
39. Y. Bai, B. Chen, F. Xiang, J. Zhou, H. Wang, Z. Suo, Transparent hydrogel with enhanced water retention capacity by introducing highly hydratable salt. *Appl. Phys. Lett.* **105**, 151903 (2014).
40. J. F. Martucci, R. A. Ruseckaite, Biodegradation behavior of three-layer sheets based on gelatin and poly (lactic acid) buried under indoor soil conditions. *Polym. Degrad. Stab.* **116**, 36–44 (2015).
41. J. Baier Leach, K. A. Bivens, C. W. Patrick Jr., C. E. Schmidt, Photocrosslinked hyaluronic acid hydrogels: Natural, biodegradable tissue engineering scaffolds. *Biotechnol. Bioeng.* **82**, 578–589 (2003).

Acknowledgments
Funding: This work was financially supported by the Japan Science and Technology (JST) ACCEL (grant number JPMJMI17F1), and C.W. was supported by Japan Society for the Promotion of Science (JSPS) Postdoctoral Fellowships. **Author contributions:** C.W., J.J.K., and T.S. conceived this concept. T.S. supervised the project. C.W. developed the materials and performed the characterization experiments. C.W., T.Y., and H.O. designed the EEG and SSVEP recording experiments. C.W., H.W., B.W., and H.M. performed the EEG and SSVEP experiments. C.W., M.O.G.N., and Y.W. performed the ECG and EMG recording experiments. H.W. and H.O. performed the EEG data processing and SSVEP data analysis. J.J.K. and S.L. contributed to the discussion of the data and results. C.W. and T.S. analyzed the data and wrote the manuscript. All authors were involved in the manuscript modifications. **Competing interests:** The authors declare that they have no competing interests. **Data and materials availability:** All data needed to evaluate the conclusions in the paper are present in the paper and/or the Supplementary Materials.

Submitted 16 January 2022
Accepted 5 April 2022
Published 20 May 2022
10.1126/sciadv.abo1396